Available online at www.sciencedirect.com
ScienceDirect
International Journal of Heat and Mass Transfer 51 (2008) 4506–4516
International Journal of HEAT and MASS TRANSFER
www.elsevier.com/locate/ijhmt

Numerical simulation of natural convection of nanofluid in a square enclosure: Effects due to uncertainties of viscosity and thermal conductivity

C.J. Ho *, M.W. Chen, Z.W. Li

Department of Mechanical Engineering, National Cheng Kung University, Tainan 70101, Taiwan, ROC

Received 19 February 2007
Available online 5 March 2008

Abstract

The present study aims to identify effects due to uncertainties in effective dynamic viscosity and thermal conductivity of nanofluid on laminar natural convection heat transfer in a square enclosure. Numerical simulations have been undertaken incorporating a homogeneous solid–liquid mixture formulation for the two-dimensional buoyancy-driven convection in the enclosure filled with alumina–water nanofluid. Two different formulas from the literature are each considered for the effective viscosity and thermal conductivity of the nanofluid. Simulations have been carried out for the pertinent parameters in the following ranges: the Rayleigh number, $Ra_f = 10^3$–10^6 and the volumetric fraction of alumina nanoparticles, $\phi = 0$–4%. Significant difference in the effective dynamic viscosity enhancement of the nanofluid calculated from the two adopted formulas, other than that in the thermal conductivity enhancement, was found to play as a major factor, thereby leading to contradictory results concerning the heat transfer efficacy of using nanofluid in the enclosure.

Keywords: Nanofluids; Natural convection; Thermal conductivity; Dynamic viscosity

1. Introduction

Suspensions of colloidal particles dubbed as nanofluids was pioneered by Choi [1], in which small amounts of metallic or metallic oxide nanoparticles are dispersed into water and other fluids. It has since then been shown experimentally [2–5] that nanofluids can have anomalously higher thermal conductivities than that of the base fluid, thus posing as a promising alternative for thermal applications. As revealed in the recent comprehensive reviews [6,7], over the past decade there have been tremendous attempts to identify and model mechanisms of thermal conductivity enhancement of nanofluids, including size and shape of the nanoparticles, the hydrodynamic interaction between nanoparticles and base fluid, clustering of particles, temperature or Brownian motion, and so on. It appears that the scarcity and inconsistency of the existing experimental data together with numerous competing theoretical models reflects further experimental and theoretical efforts are definitely needed. In contrast, relatively few experimental studies concerning the dynamic viscosity of the nanofluids have been reported in the literature [8,9]. The viscosity of nanofluids was found to be abnormally higher than that predicted by the classical mixture model [10], which, by implication, should be taken into account for possible applications of nanofluids as an effective heat transfer fluid.

Feasibility and efficacy of using various nanofluids for convective heat transfer enhancement have been experimentally explored mostly for forced convection heat transfer in horizontal circular tubes as exemplified in [11–14]. However, there appear some inconsistent findings concerning the forced convection characteristics of nanofluids. Pak and Cho [11] reported an increase of the Nusselt number of

* Corresponding author. Tel.: +886 6 2757575x62146; fax: +886 6 2352973.
E-mail address: cjho@mail.ncku.edu.tw (C.J. Ho).

0017-9310/$ - see front matter © 2008 Elsevier Ltd. All rights reserved.
doi:10.1016/j.ijheatmasstransfer.2007.12.019

Nomenclature

AR	aspect ratio, H/W
b	constant
C	coefficient
c_p	specific heat (J/kg K)
d_p^+	particle diameter (m)
F	factor of property ratios, $\beta^*_{mf}\rho^{*2}_{mf}c^*_{p,\,mf}$
g	gravitational acceleration (m/s^2)
H	enclosure height (m)
h	heat transfer coefficient (W/m^2 K)
k	thermal conductivity (W/m K)
m, n	exponent values in Eqs. 5d, 8, 13
Nu	Nusselt number, hW/k
Pe	Peclet number, defined in Eq. (5f)
Pr	Prandtl number, $\mu c_p/k$
Ra	Rayleigh number, $g\beta(T_h - T_c)W^3/(\alpha\nu)$
T	temperature (K)
T_r	reference temperature (K), $(T_h + T_c)/2$
u	dimensionless velocity component in the x direction, u^+W/α_m
v	dimensionless velocity component in the y direction, v^+W/α_m
W	enclosure width (m)
x, y	dimensionless Cartesian coordinates

Greek symbols

α	thermal diffusivity (m^2/s)
β	thermal expansion coefficient (K^{-1})
$\dot{\gamma}$	shear rate in Eq. (5f), $\frac{\partial u^+}{\partial y^+} + \frac{\partial v^+}{\partial x^+}$
ε	ratio of averaged heat transfer coefficient, $\bar{h}_m/\bar{h}_f$
θ	dimensionless temperature, $(T - T_r)/(T_h - T_c)$
μ	dynamic viscosity (kg/m s)
ν	kinematic viscosity (m^2/s)
ρ	density (kg/m^3)
ϕ	volume fraction of particles
ψ	dimensionless stream-function, ψ^+/α_m
ω	dimensionless vorticity, ω^+W^2/α_m

Subscripts

e	effective
f	base fluid
h	hot wall
m	nanofluid/mixture
p	particle
r	reference

Superscripts

*	property ratio
+	dimensional quantities
−	surface averaged quantities

water suspensions dispersed with Al_2O_3 and TiO_2 particles with an increase of the particle volumetric fraction beyond a critical value of 3%; otherwise, a decrease of heat transfer coefficient was found in comparison that of pure water. Xuan and Li [12] reported substantial heat transfer enhancement in a Cu–water suspension under turbulent flow regimes. In the entrance region of laminar flow regimes in a copper tube, Wen and Ding [13] found that dispersion of Al_2O_3 nanoparticles in water can result in significant enhancement of convective heat transfer which is higher than the enhancement of the effective thermal conductivity itself. On the other hand, for graphite–water suspensions in laminar flow regime Yang et al. [14] found that an increase of the measured heat transfer coefficients was lower than the enhancement of the effective thermal conductivity.

For natural convection heat transfer characteristics of nanofluids, relatively few research efforts have been undertaken. Incorporating a dispersion model similar to that for the flow through porous media, Khanafer et al. [15] presented a two-dimensional numerical simulation of natural convection of nanofluids in a vertical rectangular enclosure. Heat transfer across the enclosure was found to increase with the volumetric fraction of the copper nanoparticles in water at any given Grashof number. Similar prediction of heat transfer enhancement with suspended nanoparticles was reported in a recent numerical study [16] for natural convection heat transfer characteristics of a two-dimensional rectangular enclosure. However, contradictory results have been observed in the experimental studies [17–19] that dispersion of nanoparticles in base fluid may result in marked reduction, instead of enhancement, of natural convection heat transfer in enclosures. Pruta et al. [17] performed an experimental investigation for natural convection heat transfer of nanofluids inside a horizontal cylinder heated and cooled from the two ends, respectively. Nanoparticles of Al_2O_3 and CuO were used to form water-based nanofluids with particle volumetric fractions between 1% and 4%. Their results at the Rayleigh number between 10^6 and 10^9 revealed that heat transfer rate across the enclosure could become significantly deteriorated, depending on density and concentration of the nanoparticles, as well as the aspect ratio of the cylindrical enclosure. In particular, a decrease of around 150% and 300% of the Nusselt number was found, respectively, for the nanofluids with 4% of Al_2O_3 and CuO nanoparticles

at the Rayleigh number about 5×10^7. For a water–TiO_2 nanofluid filled in a rectangular enclosure heated from below, Wen and Ding [18] reported that for the Rayleigh number less than 10^6, the natural convection heat transfer rate increasingly decreased with the increase of particle concentration, particularly at low Rayleigh number. More recently, in an experimental study for natural convection in a vertical square enclosure filled with water–Al_2O_3 nanofluid of mass faction ranging from 0.36% to 10.04%[19], substantial heat transfer reduction was observed except the cases of the particle mass fraction not higher than 1%, for which marked heat transfer enhancement was detected though within the experimental uncertainty. For the above-mentioned disparity among the numerical predictions and experimental results concerning natural convection heat transfer efficacy of using nanofluid in enclosures, the possible contributing factors may include variations of the size and shape of particle, particle distribution, and uncertainties in the nanofluid thermophysical properties, in particular the effective thermal conductivity and dynamic viscosity. The present study aims to examine, via numerical simulations, the effects of uncertainties due to adopting different formulas for the effective thermal conductivity and dynamic viscosity of the water–Al_2O_3 nanofluid on natural convection heat transfer characteristics in a vertical square enclosure.

2. Problem statement and mathematical formulation

The flow configuration being considered here is that of a vertical rectangular enclosure with width of W and height H (Fig. 1). The enclosure is heated differentially between the two isothermal vertical walls at different temperatures of T_h and T_c, respectively. The top and bottom walls are maintained at adiabatic condition. The

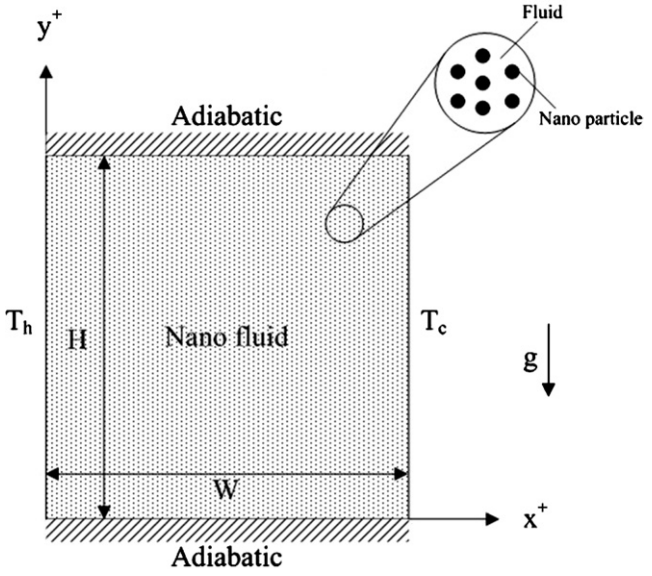

Fig. 1. Schematic for the physical configuration and coordinate system.

nanofluid in the enclosure is modeled as a dilute solid–liquid mixture with a uniform volumetric fraction ϕ of nanoparticles (Al_2O_3) dispersed within a base fluid (water). The Boussinesq approximation is assumed to be valid for the buoyancy-driven flow in the enclosure. In addition, effects of the compression work and viscous dissipation are assumed negligible.

Invoking the foregoing assumptions, the conservation of mass, momentum, and energy for the two-dimensional, laminar, steady state natural convection flow in the enclosure is expressed in terms of stream-function, vorticity and temperature. The resulting governing equations are cast in dimensionless form as follows:

Vorticity transport equation:

$$\frac{\partial(u\omega)}{\partial x}+\frac{\partial(v\omega)}{\partial y} = Pr_f\left(\frac{c^*_{p,mf}}{k^*_{mf}}\right)\left[\mu^*_{bf}\left(\frac{\partial^2\omega}{\partial x^2}+\frac{\partial^2\omega}{\partial y^2}\right)+Ra_f\rho^{*2}_{mf}\beta^*_{mf}\left(\frac{c^*_{p,mf}}{k^*_{mf}}\right)\frac{\partial\theta}{\partial x}\right] \quad (1)$$

Stream-function equation:

$$\frac{\partial^2\psi}{\partial x^2}+\frac{\partial^2\psi}{\partial y^2}=-\omega \quad (2)$$

Energy equation:

$$\frac{\partial(u\theta)}{\partial x}+\frac{\partial(v\theta)}{\partial y}=\frac{\partial}{\partial x}\left(k^*_{ef}\frac{\partial\theta}{\partial x}\right)+\frac{\partial}{\partial y}\left(k^*_{ef}\frac{\partial\theta}{\partial y}\right) \quad (3)$$

Here all spatial dimensions are normalized by the enclosure width W; all velocities are normalized by the characteristic velocity (α_m/W), α_m being the mixture thermal diffusivity of the nanofluid. The dimensionless parameters pertinent to the present problem thus include: the Rayleigh number, Ra_f and the Prandtl number, Pr_f. Also present in Eqs. (1) and (3) include the physical properties ratios of $k^*_{mf}=k_m/k_f, k^*_{ef}=k_e/k_f, \mu^*_{mf}=\mu_m/\mu_f, c^*_{p,mf}=c_{p,m}/c_{p,f}, \rho^*_{mf}=\rho_m/\rho_f$, and $\beta^*_{mf}=\beta_m/\beta_f$, where the subscripts mand f denote, respectively, the nanofluid and the base fluid. Moreover, k_e denotes the effective thermal conductivity associated with the possible heat transfer enhancement mechanisms of the nanofluid such as Brownian motion, liquid layering at liquid/particle interface, and phonon movement in nanoparticles.

The boundary conditions on these equations are specified as follows:

$$\theta=0.5, \quad \psi=0; \quad x=0 \quad (4a)$$

$$\theta=-0.5, \quad \psi=0; \quad x=1 \quad (4b)$$

$$\frac{\partial\theta}{\partial y}=0, \quad \psi=0; \quad y=0 \quad \text{or} \quad AR \quad (4c)$$

The effective thermophysical properties of the nanofluid can be evaluated using various formulas available in the literature, among which significant disparity may exist. In the present study, the focus is on the effects of uncertainties in the effective viscosity and thermal conductivity of the

nanofluid. The formulas selected for the thermophysical properties of the nanofluid in the present simulation are as follows.

Density : $$\rho_m = (1-\phi)\rho_f + \phi\rho_p \tag{5a}$$

Thermal expansion coefficient : $$\beta_m = (1-\phi)\beta_f + \phi\beta_p \tag{5b}$$

Specific heat : $$c_{p,m} = \frac{1}{\rho_m}[(1-\phi)\rho_f c_{p,f} + \phi\rho_p c_{p,p}] \tag{5c}$$

2.1. Thermal conductivity

Among the various formulas of the thermal conductivity for nanofluid presented in the literature, a correlation developed to account for the local shear effect at the liquid/particle interface in flowing suspensions [20] is adopted, which takes the form of

$$k_e = k_m(1 + b\phi Pe_p^m) \tag{5d}$$

where k_m is the mixture thermal conductivity evaluated from the well-known Maxwell formula as

$$k_m = k_f\left[\frac{2 + k_{pf}^* + 2\phi(k_{pf}^* - 1)}{2 + k_{pf}^* - \phi(k_{pf}^* - 1)}\right] \tag{5e}$$

with $k_{pf}^* = k_p/k_f$. The particle Peclet number Pe_p is defined based on the local shear rate $\dot{\gamma}$ and the particle diameter d_p^+ as

$$Pe_p = \frac{d_p^+ 2\dot{\gamma}}{\alpha_f} \tag{5f}$$

The constant b and exponent value m in Eq. (5d) depend on the particle Peclet number as given in [20].

2.2. Dynamic viscosity

For the effective dynamic viscosity of nanofluid, Brinkman's formula [10], which was adopted in the previous numerical studies [15,16], and an empirical correlation by Maïga et al. [21] are considered here and can be, respectively, expressed as

$$\mu_m = \mu_f(1-\phi)^{-2.5} \tag{5g}$$

and

$$\mu_m = \mu_f(1 + 7.3\phi + 123\phi^2) \tag{5h}$$

As illustrated in Fig. 2, with increasing particle volumetric fraction there exists increasingly great disparity between the enhancement in effective dynamic viscosity of the nanofluid calculated by Eq. (5g) and (5 h). For the nanofluid of $\phi = 4\%$, about 50% of the viscosity enhancement is estimated by Eq. (5h) while only 10% by Eq. (5g). Different nanofluid models based on a combination of the different formulas for the dynamic viscosity and thermal conductivity adopted are thus designated as shown in Table 1. As

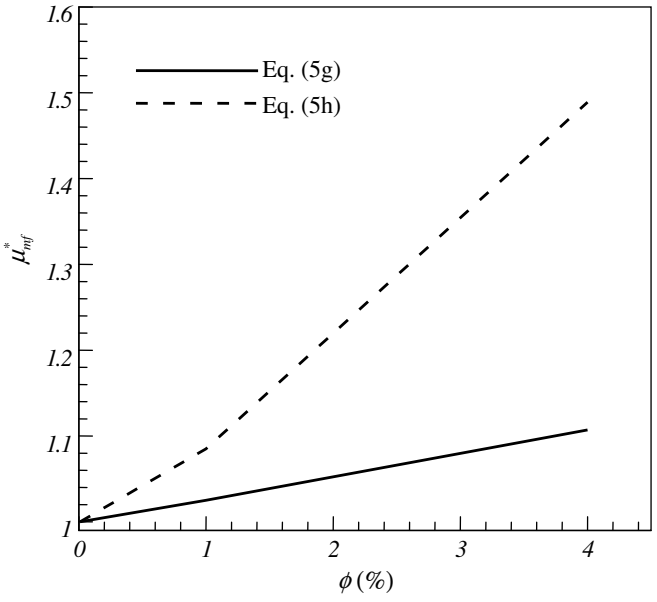

Fig. 2. Comparison of the two formulas adopted for dynamic viscosity enhancement.

Table 1
Models of nanofluid based on different formulas for thermal conductivity and dynamic viscosity

Model	Thermal conductivity ratio, k_{ef}^*	Dynamic viscosity ratio, μ_{mf}^*
I	$k_{ef}^* = k_{mf}^* = \left[\frac{2+k_{pf}^*+2\phi(k_{pf}^*-1)}{2+k_{pf}^*-\phi(k_{pf}^*-1)}\right]$	$\mu_{mf}^* = (1-\phi)^{-2.5}$
II	$k_{ef}^* = k_{mf}^* = \left[\frac{2+k_{pf}^*+2\phi(k_{pf}^*-1)}{2+k_{pf}^*-\phi(k_{pf}^*-1)}\right]$	$\mu_{mf}^* = (1+7.3\phi+123\phi^2)$
III	$k_{ef}^* = k_{mf}^*(1+b\phi Pe_p^m)$	$\mu_{mf}^* = (1-\phi)^{-2.5}$
IV	$k_{ef}^* = k_{mf}^*(1+b\phi Pe_p^m)$	$\mu_{mf}^* = (1+7.3\phi+123\phi^2)$

such, with respect to the base fluid, the models II and IV have higher effective dynamic viscosity than models I and III; while models III and IV are expected to have higher effective thermal conductivity than models I and II.

The local and averaged heat transfer rates at the hot wall of the enclosure are presented by means of the local and averaged Nusselt numbers, $Nu_{h,f}$ and $\overline{Nu}_{h,f}$, which are, respectively, evaluated as follows

$$Nu_{h,f} = \frac{h_m W}{k_f} = -k_{ef}^*\left.\frac{\partial\theta}{\partial x}\right|_{x=0} \tag{6a}$$

$$\overline{Nu}_{h,f} = \frac{\bar{h}_m W}{k_f} = \frac{1}{AR}\int_0^{AR}\left(-k_{ef}^*\left.\frac{\partial\theta}{\partial x}\right|_{x=0}\right)dy \tag{6b}$$

Furthermore, to quantify heat transfer efficacy of using nanofluid, a ratio of the averaged heat transfer coefficient at the hot wall to that of the base fluid, ε_h, is evaluated as

$$\varepsilon_h = \bar{h}_m/\bar{h}_f \tag{7}$$

The natural convection heat transfer rate across an enclosure may be generally expressed as a correlation of the averaged Nusselt number $\overline{Nu}_{h,m}$ with the Rayleigh number Ra_m in the form of

$$\overline{Nu}_{\mathrm{h,\,m}} = \frac{\bar{h}_{\mathrm{m}} W}{k_{\mathrm{m}}} = CRa_{\mathrm{m}}^{n} = C\left(\frac{g\rho_{\mathrm{m}}^{2} c_{\mathrm{p,\,m}} \beta_{\mathrm{m}} \Delta T W^{3}}{\mu_{\mathrm{m}} k_{\mathrm{m}}}\right)^{n} \tag{8}$$

where the coefficient C and exponent n are constants. A relation of the heat transfer coefficient with the relevant physical properties under the conditions of a fixed temperature difference $\Delta T(=T_{\mathrm{h}} - T_{\mathrm{c}})$ across an enclosure of fixed characteristic dimension W can thus be written as

$$\bar{h}_{\mathrm{m}} \sim \beta_{\mathrm{m}}^{n} \rho_{\mathrm{m}}^{2n} c_{\mathrm{p,\,m}}^{n} k_{\mathrm{m}}^{1-n} \mu_{\mathrm{m}}^{-n} \tag{9}$$

A relation of the heat transfer coefficient ratio ε_{h} in Eq. (7) with the thermophysical property ratios between the nanofluid and the base fluid may be accordingly postulated as

$$\varepsilon_{\mathrm{h}} \sim (\beta_{\mathrm{mf}}^{*})^{n} (\rho_{\mathrm{mf}}^{*})^{2n} (c_{\mathrm{p,\,mf}}^{*})^{n} (k_{\mathrm{mf}}^{*})^{1-n} (\mu_{\mathrm{mf}}^{*})^{-n} \tag{10}$$

In view of the fact that the four models in Table 1 have the same formulas for the density, specific heat, and thermal expansion coefficient, the relation of Eq. (10) can be rearranged into

$$\varepsilon_{\mathrm{h}} \sim F^{n} (k_{\mathrm{mf}}^{*})^{1-n} (\mu_{\mathrm{mf}}^{*})^{-n} \tag{11}$$

where the factor $F(=\beta_{\mathrm{mf}}^{*} \rho_{\mathrm{mf}}^{*2} c_{\mathrm{p,\,mf}}^{*})$, as shown in Fig. 3, has a value of increasingly higher than unity with increasing volumetric particle fraction, primarily stemming from the corresponding enhanced density of the nanofluid. In contrast, with respect to that of the base fluid, the thermal expansion coefficient as well as the specific heat of the nanofluid, also plotted in Fig. 3, exhibits a marked decrease with the particle fraction, thereby might inducing detrimental influence on the heat transfer coefficient. Moreover, it can be inferred from Eq. (11) that for $0 < n < 1$ as generally expected, enhancements in both effective thermal conductivity and dynamic viscosity of the nanofluid can be expected to play mutually counteracting roles so as to exert beneficial and detrimental influences on the heat transfer coefficient ratio, respectively.

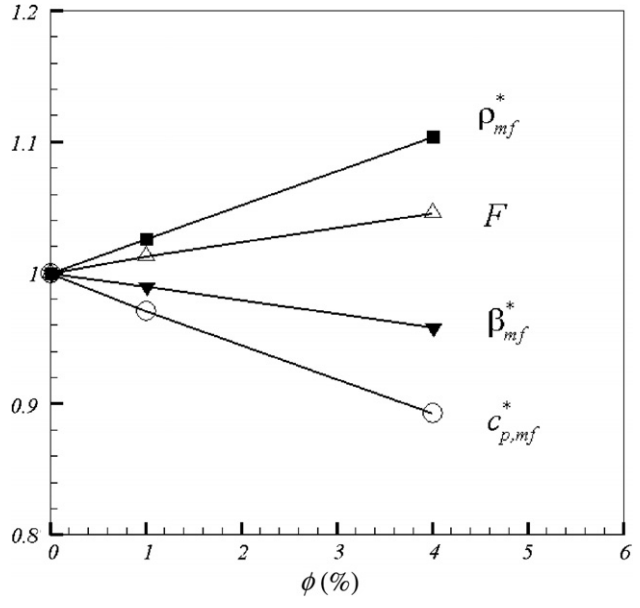

Fig. 3. Variations of the property ratio factor F, the density ratio ρ_{mf}^{*}, the thermal expansion coefficient ratio β_{mf}^{*}, and the specific heat ratio $c_{\mathrm{p,\,mf}}^{*}$ with the particle volumetric fraction.

Table 2
Comparison of results for averaged Nusselt number in an air-filled square enclosure at different Rayleigh numbers

Ra_{f}	$\overline{Nu}_{\mathrm{h}}$		
	Present	De Vahl Davis [22]	Fusegi et al. [23]
10^3	1.118	1.118	1.106
10^4	2.246	2.238	2.302
10^5	4.522	4.509	4.646
10^6	8.825	8.817	9.012

3. Numerical method

The dimensionless governing equations, Eqs. (1) and (3), together with the boundary conditions, Eq. (4), were discretized using a finite volume method. The QUICK and central differencing schemes were, respectively, used to approximate convection and diffusion terms in the differential equations. The solution domain is discretized with a mesh with non-uniform spacing in the horizontal direction with grids clustering toward the vertical walls, which allows the boundary layers to be resolved without an excessive number of grids. The grid spacing along the width of the enclosure is distributed according to the following equation:

$$g(x) = 0.5 + \frac{\tan(2x-1)\eta}{\tan\eta} \tag{12}$$

where η is a grid clustering parameter with $0 < \eta < (\pi/2)$.

The resulting system of discretized equations was solved iteratively in a line-by line manner in conjunction with relaxation technique. The iteration was terminated when a relative convergence criterion of 10^{-6} was met by all the variables. The integral energy balance across the enclosure for the converged solutions was also checked to be within 0.5%.

The numerical code is validated against the benchmark results [22,23] for natural convection in an air-filled square enclosure at different Rayleigh numbers as shown in Table 2. An excellent agreement is apparently displayed between the present results and the benchmark solutions for the averaged Nusselt number at the hot wall of the

Table 3
Thermophysical properties of base fluid and nanoparticles

Property	Base fluid (water)	Nanoparticle (Al_2O_3)
c_{p} (J/kg K)	4179	765
ρ (kg/m^3)	997.1	3600
k (W/m K)	0.605	46
μ (kg/m s)	8.91×10^{-4}	–
β (K^{-1})	2.1×10^{-4}	6.3×10^{-6}

enclosure. To ensure the grid convergence of the numerical solutions, different meshes varying from 61×61 to 161×161 have been tested. Simulation results shown later have been obtained for several meshes ranging from 81×81 to 121×121, depending mainly on the Rayleigh number.

4. Results and discussion

The working nanofluid in the enclosure is chosen as alumina (Al_2O_3) – water mixture. The thermophysical properties of the base fluid (water) and nanoparticles (Al_2O_3) are tabulated in Table 3. Numerical simulation

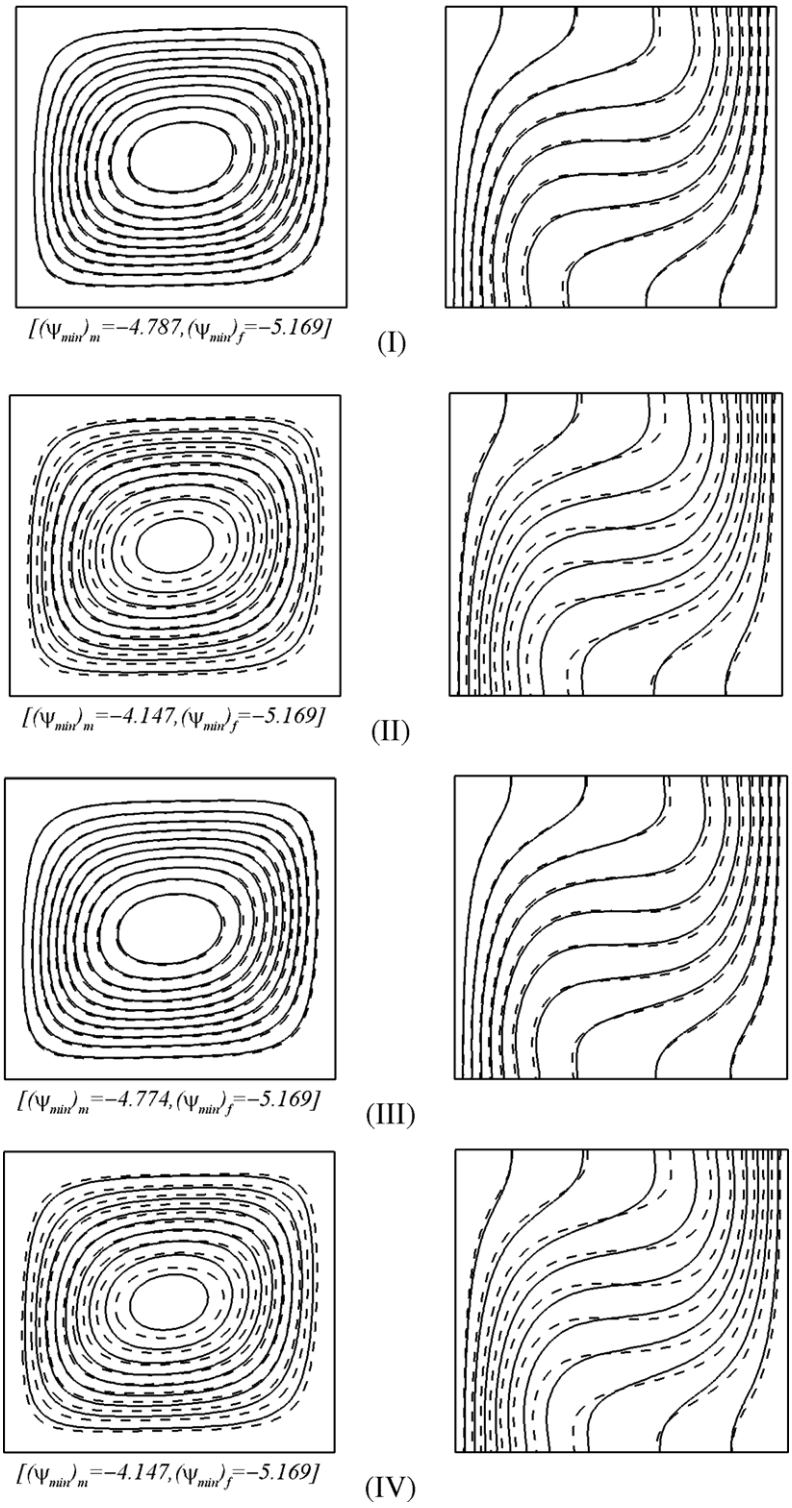

Fig. 4. Comparison of the streamlines (left) and isotherms (right) contours between nanofluids (—) ($\phi = 4\%$) and base fluid (- - -) ($\phi = 0\%$) at $Ra_f = 10^4$ for different models.

has been carried out for a square enclosure, $AR = 1$, with the relevant parameters in the following values and ranges: $Ra_f = 10^3$–10^6, $Pr_f = 6.2$, and the volumetric fraction of alumina nanoparticles, $\phi = 0$–4%. In the following, numerical results obtained incorporating variant models tabulated in Table 1 for the nanofluid are presented to explore the effects of uncertainties associated with various formulas for effective thermal conductivity and dynamic viscosity on the heat transfer characteristics in the enclosure.

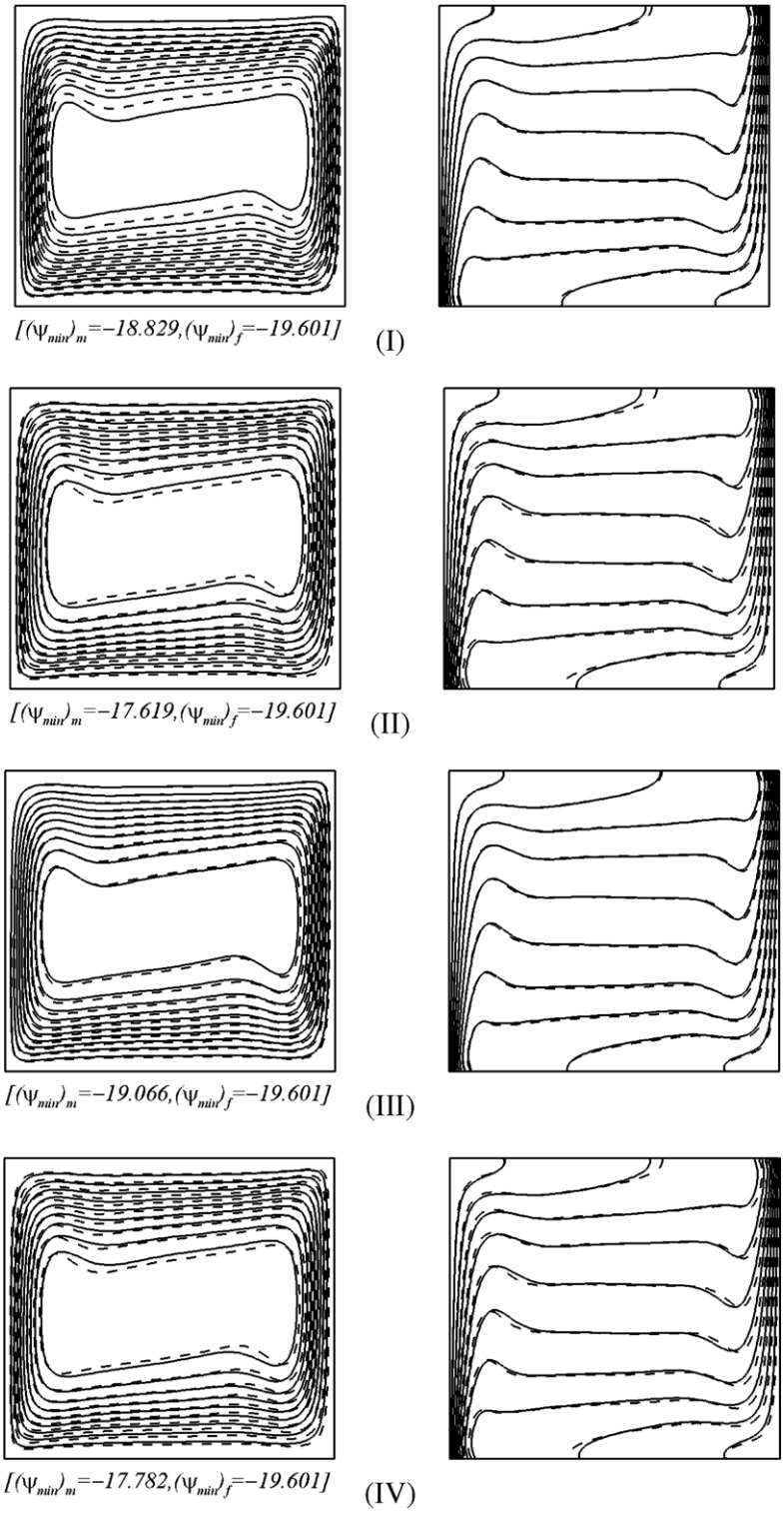

Fig. 5. Comparison of the streamlines (left) and isotherms (right) contours between nanofluids (—)($\phi = 4\%$) and base fluid (---)($\phi = 0\%$) at $Ra_f = 10^6$ for different models.

For all models the buoyancy-driven flow in the enclosure at a fixed Rayleigh number tends to weaken with an increase in the volumetric fraction of nanoparticles.

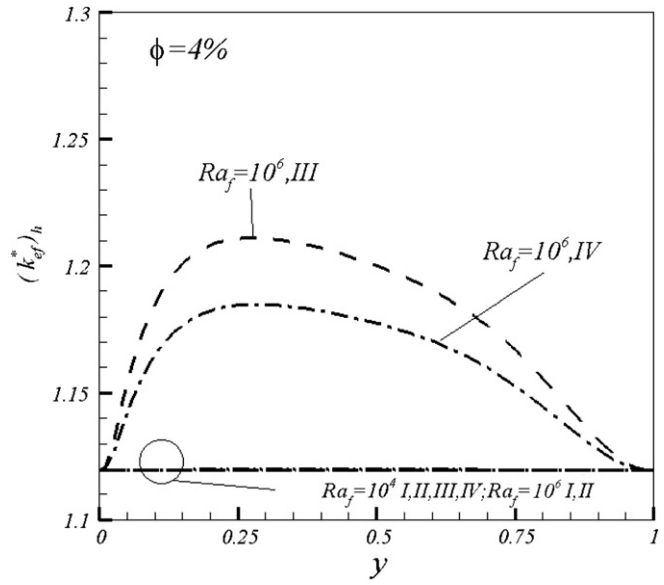

Fig. 6. Enhancement of effective thermal conductivity due to local shear rate along the hot wall of the enclosure with nanofluid of $\phi = 4\%$.

Figs. 4 and 5 illustrate comparison of the streamlines and isotherms contours between the nanofluid ($\phi = 4\%$) based on the four models and the base fluid ($\phi = 0\%$) at two values of $Ra_f = 10^4$ and 10^6, respectively. Specifically, for the models II and IV which have significantly higher viscosity enhancement, a reduction of more than 23% and 11% in the extreme values of the stream-function can be detected for the nanofluid compared with those for the base fluid, respectively, at $Ra_f = 10^4$ and 10^6. In the presence of the weaker buoyant flow, the clustering of the isotherms along the thermally active walls of the enclosure appears rather loosen particularly for $Ra_f = 10^4$ as shown in Fig. 4.

Fig. 6 illustrates the thermal conductivity enhancement along the hot wall due to local shear effect accounted in models III and IV for the nanofluid of $\phi = 4\%$ at $Ra_f = 10^4$ and 10^6. The effective thermal conductivity becomes further augmented at the hot wall in the presence of intensified buoyancy-driven flow at $Ra_f = 10^6$ for the models III and IV relative to that for the models I and II; while appears essentially unaffected at $Ra_f = 10^4$ for all models. Similar observation can be made for the surface averaged effective thermal conductivity enhancement of the nanofluid, as shown in Fig. 7 for different models at various particle fractions and Rayleigh numbers. Specifically, the highest enhancement in the effective thermal conductiv-

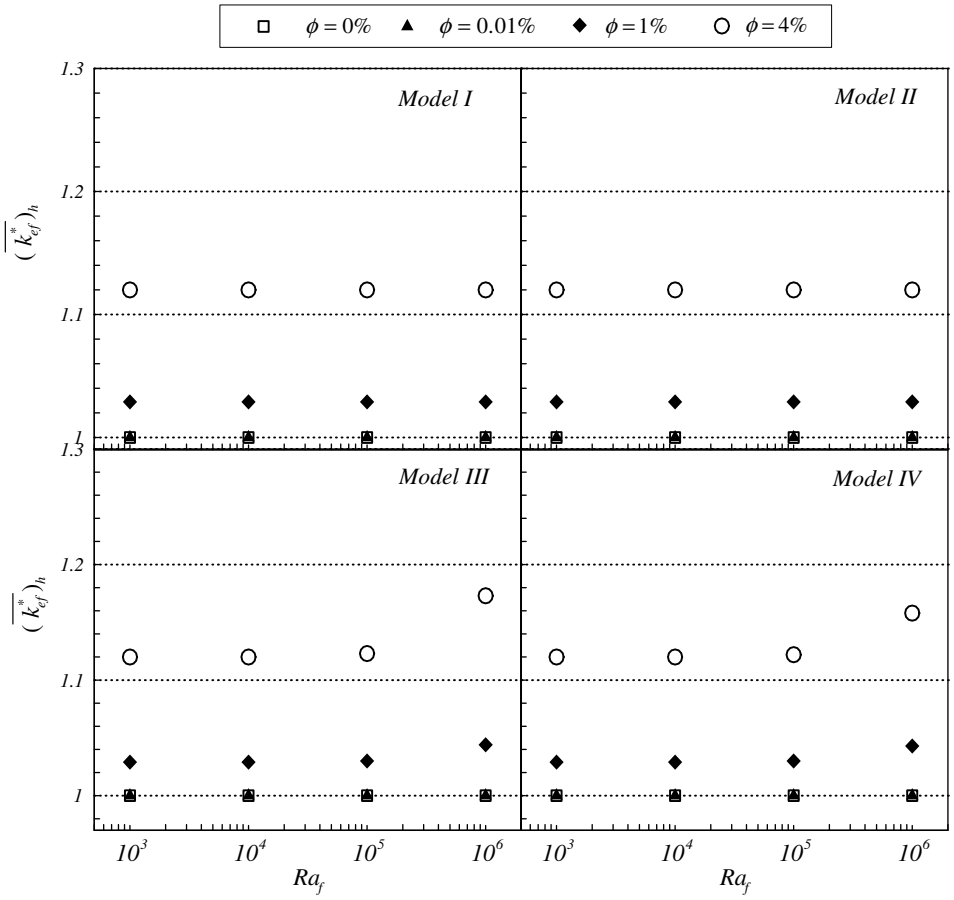

Fig. 7. Surface averaged effective thermal conductivity ratio at the hot wall for nanofluid of different models.

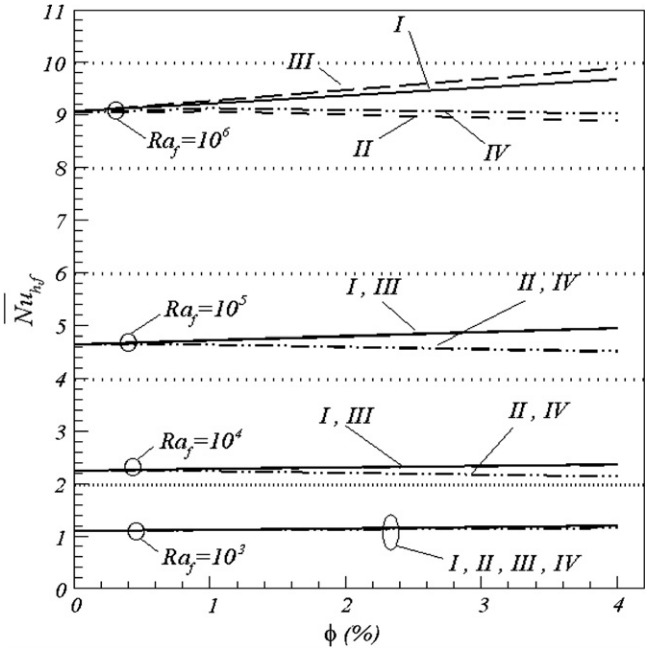

Fig. 8. Variation of averaged Nusselt number with volumetric fraction for different models.

ity over the hot wall is found to be more than 17% at $Ra_f = 10^6$ for $\phi = 4\%$ of the model III. Nevertheless, it should be noted that such magnitude of enhancement in the effective thermal conductivity appears considerably lower than that in the dynamic viscosity attained using the empirical formula of Eq. (5h), lending the latter to act possibly as a major factor for heat transfer efficacy of the nanofluid as to be elaborated later.

Next, the averaged Nusselt number at the hot wall $\overline{Nu}_{h,f}$ is presented in Fig. 8 for the various models of the nanofluid. For all models at various Rayleigh numbers the averaged Nusselt number exhibits a monotonic variation with the volumetric fraction of nanoparticles. A further scrutiny of the curves in Fig. 8, however, reveals that in contrast to the numerical results in [15,16], using the nanofluid in the enclosure does not always result in an increase of the averaged Nusselt number, depending mainly on the Rayleigh number as well as the formulas for the effective dynamic viscosity. At $Ra_f = 10^3$ under which conduction heat transfer dominates across the enclosure, an increase in the averaged Nusselt number with increasing particle fraction can be seen to occur for all the models, reflecting the beneficial effect due to enhancement in thermal conductivity of the nanofluid. At the higher values of Ra_f ($\geqslant 10^4$) with the corresponding increasingly convection-dominated heat transfer across the enclosure, the difference between the effective dynamic viscosity enhancement of the nanofluid calculated using the two adopted formulas comes into play as a major factor, such that the curves of the averaged Nusselt number shown in Fig. 8 exhibit a decreasing and increasing trend with the particle fraction, respectively, for two groups of models: (II & IV) and (I & III), between which the formulas adopted for the dynamic viscosity differ. The detrimental/beneficial effects of the particle fraction on the averaged Nusselt number tend to become further pronounced with increasing Rayleigh number. Particularly, at $Ra_f = 10^6$, as can be discerned in Fig. 8, the upward/downward curves with the increasing particle fraction, respectively, for model III/IV, further promoted by the implicit enhancement in the thermal conductivity due to the local shear illustrated in Figs. 6 and 7, becomes increasingly deviated from those for model I/II, so that the models III and II attain the highest and lowest averaged Nusselt number at fixed particle fraction. The foregoing contradictory behaviors of the averaged Nusselt number primarily dictated by the significant difference between the dynamic viscosity enhancements calculated using the two adopted formulas might contribute to explaining the disparate findings among the numerical predictions [15,16] and experimental results [17–19] in the literature concerning heat transfer efficacy of using nanofluid for natural convection in enclosures. Moreover, the averaged Nusselt number at the hot wall obtained from the four models under consideration can be, respectively, correlated pretty well with the Rayleigh number ($10^4 \leqslant Ra_f \leqslant 10^6$) and the volumetric particle fraction ($0 \leqslant \phi \leqslant 0.04$) as follows:

$$\overline{Nu}_{h,f} = C(1+\phi)^m Ra_f^n \tag{13}$$

where the coefficient C and the exponents m, n for each model are tabulated in Table 4. The positive and negative values for the exponent m tabulated in Table 4 for various models further reflect the beneficial and detrimental effects predicted from the respective nanofluid model on the natural convection heat transfer across the enclosure.

Finally, the heat transfer efficacy of the nanofluid can be further delineated from the results of the heat transfer coefficient ratio ε_h plotted in Fig. 9 for various models, respectively. An overview of the figures clearly reveals that under the situation of conduction-dominated heat transfer across the enclosure at $Ra_f = 10^3$, the beneficial effect of using nanofluid as the heat transfer medium is further

Table 4
Values of coefficient C and exponents m, n for different models

Model	C	M	n	Maximum deviation	Average deviation	Correlation coefficient
I	0.149	1.624	0.297	5.65%	1.59%	0.999
II	0.148	−0.561	0.298	4.63%	1.63%	0.999
III	0.145	2.067	0.300	4.58%	1.54%	0.999
IV	0.145	−0.261	0.300	5.65%	1.59%	0.999

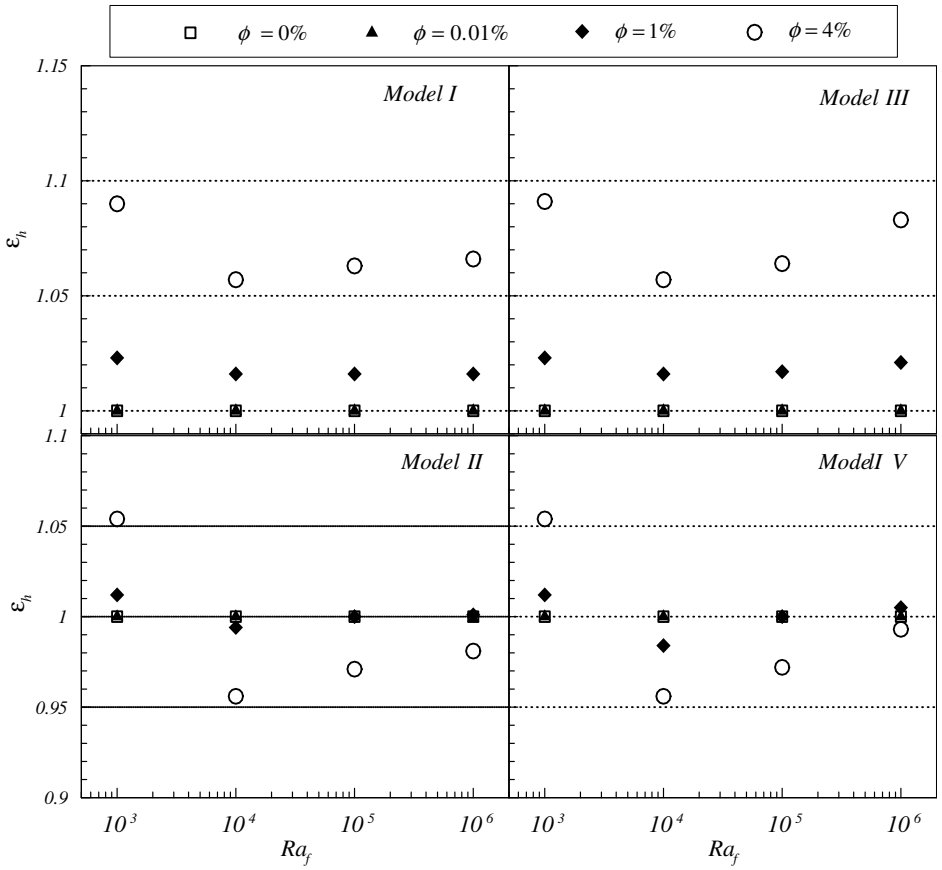

Fig. 9. Heat transfer coefficient ratio for nanofluid of different models.

demonstrated for all models, consistent with that displayed in Fig. 8. Increasing the particle fraction up to 4% at $Ra_f = 10^3$, for instance, can induce an increase of 9% in the averaged heat transfer coefficient of the nanofluid with respect to the base fluid, as shown in Fig. 9 for models I and III. As the Rayleigh number is increased to 10^4, however, the heat transfer coefficient ratio for a fixed particle fraction appears substantially reduced, depending primarily on the effective viscosity enhancement in each model. Specifically, the heat transfer coefficient ratio drastically drops to below unity for models II and IV while markedly decreases but remains above unity for models I and III, particularly for the nanofluid of high particle fraction. For the nanofluid of $\phi = 4\%$ at $Ra_f = 10^4$, for instance, the heat transfer coefficient ratio decreases to 1.057 and 0.956 for models III and II, respectively. Moreover, an increase in the Rayleigh number beyond 10^4 tends to attenuate/magnify, respectively, the above-mentioned heat transfer mitigation/ enhancement effects of the nanofluid, as indicated by the noticeable uplift of the heat transfer coefficient ratio for all models shown in Fig. 9. In particular, with an increase of Ra_f up to 10^6 for the nanofluid of $\phi = 4\%$, models II and III have the lowest and highest heat transfer coefficient ratios of 0.981 and 1.083, respectively, in conformity with that revealed in Fig. 8 as well.

5. Concluding remarks

In this article, the influences of uncertainties due to adopting various formulas for the effective thermal conductivity and dynamic viscosity of alumina–water nanofluid on the heat transfer characteristics have been investigated numerically for natural convection in a square vertical enclosure. Simulation results from a comparative study of four different models based on two different formulas, respectively, for the effective thermal conductivity and dynamic viscosity of the nanofluid have been presented in detail. Results clearly demonstrate that the uncertainties associated with different formulas adopted for the effective thermal conductivity and dynamic viscosity of the nanofluid have a strong bearing on the natural convection heat transfer characteristics in the enclosure. Significant difference between enhancements in the dynamic viscosity estimated from the two adopted formulas leads to contradictory heat transfer efficacy of the nanofluid, so that the heat transfer across the enclosure can be found to be enhanced or mitigated with respect to the base fluid. Enhancement in the dynamic viscosity, counteracting that in the thermal conductivity, of the nanofluid can thus play as a crucial factor and should be taken into account when accessing its heat transfer efficacy for natural convection in enclosures.

Acknowledgements

The authors wish to thank the National Science Council of ROC in Taiwan for the financial support to present study through the Projects: NSC93-2212-E006-013, NSC94-2212-E006-101, and NSC95-2212-E006-232. The constructive comments from the reviewers are greatly appreciated.

References

[1] S.U.S. Choi, Enhancing thermal conductivity of fluids with nanoparticles, in: ASME FED, vol. 231, 1995, pp. 99–105.
[2] J.A. Eastman, S.U.S. Choi, S. Li, W. Yu, L.J. Thompson, Anomalously increased effective thermal conductivities of ethylene glycol-based nanofluids containing copper nanoparticles, Appl. Phys. Lett. 78 (2001) 718–720.
[3] S. Lee, S.U.S. Choi, J.A. Eastman, Measuring thermal conductivity of fluids containing oxide nanoparticles, J. Heat Transfer 121 (1999) 280–289.
[4] Y.M. Xuan, Q. Li, Heat transfer enhancement of nanofluids, Int. J. Heat Fluid Flow 21 (2000) 58–64.
[5] H. Xie, J. Wang, T.G. Xie, Y. Liu, F. Ai, Thermal conductivity enhancement of suspensions containing nanosized alumina particles, J. Appl. Phys. 91 (2002) 4568–4572.
[6] S.K. Das, S.U.-S. Choi, H.E. Patel, Heat transfer in nanofluids – a review, Heat Transfer Eng. 37 (2006) 3–19.
[7] X.Q. Wang, A.S. Mujumdar, Heat transfer characteristics of nanofluids: a review, Int. J. Thermal Sci. 46 (2007) 1–19.
[8] X. Wang, X. Xu, S.U.S. Choi, Thermal conductivity of nanoparticles–fluid mixture, J. Thermophys. Heat Transfer 13 (1999) 474–480.
[9] S.K. Das, N. Patel, W. Roetzel, Pool boiling characteristics of nanofluids, Int. J. Heat Mass Transfer 46 (2003) 851–862.
[10] H.C. Brinkman, The viscosity of concentrated suspensions and solution, J. Chem. Phys. 20 (1952) 571–581.
[11] B.C. Pak, Y.I. Cho, Hydrodynamic and heat transfer study of dispersed fluids with submicron metallic oxide particles, Exp. Heat Transfer 11 (1999) 151–170.
[12] Y.M. Xuan, Q. Li, Investigation on convective heat transfer and flow features of nanofluids, J. Heat Transfer 125 (2003) 151–155.
[13] D.S. Wen, Y.L. Ding, Experimental investigation into convective heat transfer of nanofluids at entrance area under laminar flow region, Int. J. Heat Mass Transfer 47 (2004) 5181–5188.
[14] Y. Yang, Z. Zhang, E. Grulke, W. Anderson, G. Wu, Heat transfer properties of nanoparticle-in-fluid dispersions (nanofluids) in laminar flow, Int. J. Heat Mass Transfer 48 (2005) 1107–1116.
[15] K. Khanafer, K. Vafai, M. Lightstone, Buoyancy-driven heat transfer enhancement in a two-dimensional enclosure utilizing nanofluids, Int. J. Heat Mass Transfer 46 (2003) 3639–3653.
[16] X.Q. Wang, A.S. Mujumdar, C. Yap, Free convection heat transfer in horizontal and vertical rectangular cavities filled with nanofluids, in: Proceedings of the 13th International Heat Transfer Conference, Sydney, Australia, 2006.
[17] N. Pruta, W. Roetzel, S.K. Das, Natural convection of nano-fluids, Heat Mass Transfer 39 (2003) 775–784.
[18] D. Wen, Y. Ding, Formulation of nanofluids for natural convective heat transfer applications, Int. J. Heat Fluid Flow 26 (2005) 855–864.
[19] C.J. Ho, C.C. Lin, Experiments on natural convection heat transfer of a nanofluid in a square enclosure, in: Proceedings of the 13th International Heat Transfer Conference, Sydney, Australia, 2006.
[20] P. Charuyakorn, S. Sengupta, S.K. Roy, Forced convection heat transfer in microencapsulated phase change material slurries, Int. J. Heat Mass Transfer 34 (1991) 819–833.
[21] S.E.B. Maïga, C.T. Nguyen, N. Galanis, G. Roy, Heat transfer enhancement in forced convection laminar tube flow by using nanofluids, in: Proceedings of International Symposium on Advances in Computational Heat Transfer III, Paper CHT-040101, 2004, p. 24.
[22] G. De Vahl Davis, Natural convection of air in a square cavity, a benchmark numerical solution, Int. J. Numer. Methods Fluids 3 (1962) 249–264.
[23] T. Fusegi, J.M. Hyun, K. Kuwahara, B. Farouk, A numerical study of three-dimensional natural convection in a differentially heated cubical enclosure, Int. J. Heat Mass Transfer 34 (1991) 1543–1557.